

# Efficient reduction of NO<sub>x</sub> by H<sub>2</sub> under oxygen-rich conditions over Pd/TiO<sub>2</sub> catalysts: an *in situ* DRIFTS study

Norman Macleod, Rachael Cropley, and Richard M. Lambert \*

Department of Chemistry, University of Cambridge, Lensfield Road, Cambridge CB2 1EW, UK

Received 8 October 2002; accepted 14 November 2002

The H<sub>2</sub>/NO/O<sub>2</sub> reaction under lean-burn conditions has been studied by means of *in situ* DRIFTS, reactor measurements and temperature-programmed desorption with the aim of understanding the very different behavior of Pd/TiO<sub>2</sub> and Pd/Al<sub>2</sub>O<sub>3</sub> catalysts. The former deliver very high NO<sub>x</sub> conversions (70–80%) with good N<sub>2</sub> selectivity whereas the latter show very low activity. In addition, Pd/TiO<sub>2</sub> exhibits two distinct NO<sub>x</sub> reduction pathways, thus greatly extending the useful temperature range. It is shown that the Pd/TiO<sub>2</sub> low-temperature channel involves adsorption and subsequent dissociation of NO on reduced (Pd<sup>0</sup>) metal sites. The low activity of Pd/Al<sub>2</sub>O<sub>3</sub> is a consequence of palladium remaining in an oxidized state under reaction conditions. The high-temperature NO reduction channel found with Pd/TiO<sub>2</sub> is associated with the generation and subsequent reaction of NH<sub>x</sub> species.

**KEY WORDS:** NO; palladium; H<sub>2</sub>; N<sub>2</sub>O; lean burn; Al<sub>2</sub>O<sub>3</sub>; TiO<sub>2</sub>; FTIR; DRIFTS.

## 1. Introduction

The large oxygen excess present in exhaust streams generated by lean-burn gasoline and diesel engines makes effective utilization of any reductant species present (HC, CO, H<sub>2</sub>) for NO<sub>x</sub> reduction extremely difficult [1–4]. The lack of a suitable catalyst/reductant combination for this process is a major obstacle preventing widespread introduction of fuel-efficient lean-burn engines, which have the potential to reduce significantly the global CO<sub>2</sub> burden. The control of NO<sub>x</sub> emissions from stationary power sources and various chemical plants is also environmentally important. For these applications the NH<sub>3</sub> SCR process [3,4] is currently the preferred option for NO<sub>x</sub> removal. Although the process is very effective, the requirement for a separate NH<sub>3</sub> source and injection system disfavors the use of this technology for mobile applications.

A large body of work already exists regarding lean NO<sub>x</sub> reduction with hydrocarbons. Under these conditions platinum-based catalysts are amongst the most active, delivering useful NO<sub>x</sub> conversion in a temperature window typically between 200 and 300 °C [5,6]. Recently, several authors have also investigated the use of hydrogen as a reductant with platinum-based catalysts [7–12]. These studies indicate that hydrogen is a promising reductant for lean NO<sub>x</sub> control, delivering NO<sub>x</sub> conversions in the region of 60–80% at temperatures of 90–150 °C [7–12]. However, the nitrogen selectivity of the H<sub>2</sub>/NO/O<sub>2</sub> reaction over platinum is low, tending to produce more N<sub>2</sub>O than N<sub>2</sub>.

Much less attention has been directed toward palladium-based catalysts. Burch and Coleman [10] studied both Pd/Al<sub>2</sub>O<sub>3</sub> and Pt/Al<sub>2</sub>O<sub>3</sub> catalysts. The palladium catalyst was found to exhibit very low activity for NO<sub>x</sub> reduction with hydrogen as the reductant. The authors speculated that this could have been due to palladium remaining in an oxidized state under reaction conditions, in contrast to the significantly more active (and presumably fully reduced) platinum catalyst. Palladium catalysts on various supports were investigated by Ueda *et al.* for the H<sub>2</sub>/NO/O<sub>2</sub> reaction under lean-burn conditions in the presence of 10% H<sub>2</sub>O [9,13]. They found significant support-mediated effects. Thus with Pd/Al<sub>2</sub>O<sub>3</sub> the maximum NO<sub>x</sub> conversion obtained was below 10%, but with Pd/TiO<sub>2</sub> this increased dramatically to >50% [13]. However, no explanation of these effects was offered.

In the present study we have investigated the H<sub>2</sub>/NO/O<sub>2</sub> reaction over both Pd/TiO<sub>2</sub> and Pd/Al<sub>2</sub>O<sub>3</sub> catalysts, with the aim of elucidating the phenomena responsible for the vastly superior performance of Pd/TiO<sub>2</sub>. *In situ* DRIFTS and temperature-programmed desorption (TPD) were employed to characterize the adsorbed species present under reaction conditions. With Pd/TiO<sub>2</sub> clear evidence is found for the presence of metallic palladium under reaction conditions, accounting for the high activity of this catalyst, whilst for Pd/Al<sub>2</sub>O<sub>3</sub> the metal remains predominantly in an oxidized state. A high-temperature NO<sub>x</sub> reduction pathway is also observed on Pd/TiO<sub>2</sub>, which operates via NH<sub>x</sub> intermediates.

## 2. Experimental

The 0.5 wt% Pd/γ-Al<sub>2</sub>O<sub>3</sub> and 0.5 wt% Pd/TiO<sub>2</sub> catalysts were prepared by impregnation of alumina (Aldrich)

\* To whom correspondence should be addressed.  
E-mail: rml1@cam.ac.uk

and titania (Degussa P25) carriers with aqueous solutions of palladium(II) nitrate (Aldrich). Following impregnation the catalysts were dried in air overnight at 110 °C, calcined in air at 500 °C and subsequently crushed/sieved to yield grain sizes in the range 255–350 μm. Metal dispersion was determined using the CO methanation technique [14,15], assuming a 1:1 CO to surface metal atom ratio. The dispersions measured were 47 and 30% for Pd/γ-Al<sub>2</sub>O<sub>3</sub> and Pd/TiO<sub>2</sub> respectively.

Catalyst testing was performed in a quartz micro-reactor system described previously [12]. The feed composition employed contained 4000 ppm H<sub>2</sub>, 500 ppm NO and 5% O<sub>2</sub>, delivered to the reactor with a total flow of 200 ml min<sup>-1</sup>. A sample weight of 100 mg was employed, corresponding to a reciprocal weight time velocity of  $w/f = 0.03 \text{ g s ml}^{-1}$ . Prior to testing the samples were calcined in air (60 ml min<sup>-1</sup>) for 6 h at 500 °C. The reactor outflow was analyzed using a chemiluminescence NO<sub>x</sub> (NO + NO<sub>2</sub>) analyzer (Signal 4000 series) and a dual channel NDIR detector (Siemens Ultramat 6) calibrated for NO/N<sub>2</sub>O. Hydrogen consumption was monitored via a quadrupole mass spectrometer (Hiden RGA 301). Nitrogen production was calculated by subtracting the N<sub>2</sub>O contribution from the total NO<sub>x</sub> conversion (GC analysis produced no evidence for NH<sub>3</sub> in the reactor outlet during these experiments). The catalyst temperature and all analyzer outputs were continuously monitored and recorded by PC-based software. Light-off profiles, typically containing 1000 data points per channel, were obtained as the catalyst temperature was raised from 50 to 450 °C with a linear ramp of 2 K min<sup>-1</sup>. TPD experiments were also performed in this system, employing a He flow of 150 ml min<sup>-1</sup> with a heating rate of 10 K min<sup>-1</sup>. The sample (100 mg) was calcined at 500 °C, cooled to 50 °C in helium and subsequently dosed with a feed containing 500 ppm NO + 5% O<sub>2</sub>. After flushing the system the TPD ramp was then performed between 50 and 550 °C. Desorption of nitrogen oxides (N<sub>2</sub>O, NO, NO<sub>2</sub>) was monitored by a combination of NDIR and chemiluminescence whilst O<sub>2</sub> and N<sub>2</sub> desorption was monitored via the mass spectrometer.

DRIFTS experiments were performed with a Perkin-Elmer GX2000 spectrometer equipped with an MCT detector and a high-temperature, high-pressure DRIFTS cell (Thermo Spectra-Tech) fitted with ZnSe windows. Spectra were acquired at a resolution of 4 cm<sup>-1</sup> typically averaging 64 scans. Background spectra were obtained from samples at the relevant temperature in a flow of helium.

### 3. Results and discussion

#### 3.1. Catalyst activity

Conversion versus temperature profiles for the reduction of NO by hydrogen (4000 ppm H<sub>2</sub> + 500 ppm

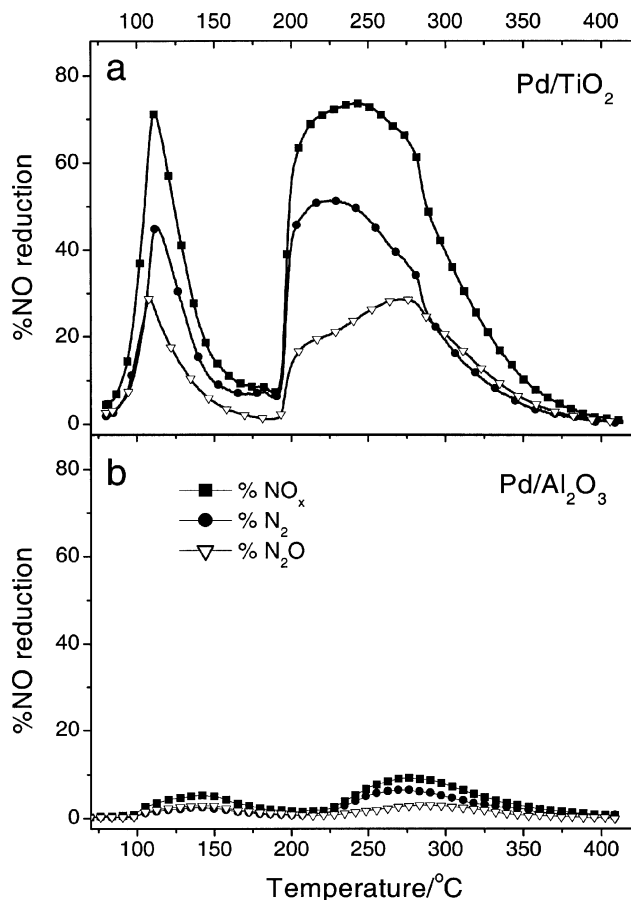


Figure 1. Total NO conversion and N<sub>2</sub>/N<sub>2</sub>O yields as a function of temperature during NO reduction by H<sub>2</sub> over (a) 0.5 wt% Pd/TiO<sub>2</sub> and (b) 0.5 wt% Pd/Al<sub>2</sub>O<sub>3</sub> (4000 ppm H<sub>2</sub> + 500 ppm NO + 5% O<sub>2</sub>).

NO + 5% O<sub>2</sub>) over 0.5 wt% Pd/TiO<sub>2</sub> and 0.5 wt% Pd/Al<sub>2</sub>O<sub>3</sub> are displayed in figures 1(a) and (b) respectively. It is apparent that the choice of support strongly influences NO<sub>x</sub> reduction under these conditions, with the TiO<sub>2</sub>-supported catalyst delivering dramatically improved NO<sub>x</sub> conversion (~70%) compared to the Al<sub>2</sub>O<sub>3</sub>-supported sample (~10%). Furthermore, as observed by Ueda *et al.* [9,13], two distinct reduction maxima are observed with Pd/TiO<sub>2</sub>, one centered at low temperature in the region where H<sub>2</sub> conversion approaches 100% (110 °C), and one at higher temperature (~240 °C). This behavior clearly indicates the operation of two separate mechanisms for NO<sub>x</sub> reduction with the titania-supported catalyst. (Although a second maximum is also discernible with Pd/Al<sub>2</sub>O<sub>3</sub>, the efficiency of this process is very much reduced compared to that on Pd/TiO<sub>2</sub>.) The TiO<sub>2</sub>-supported catalyst also gave good nitrogen selectivity (defined as  $\%S_{N_2} = [N_2]/([N_2] + [N_2O]) \times 100$ ): around 70% in the vicinity of the maxima in the NO<sub>x</sub> reduction profile.

### 3.2. Characterization of adsorbed NO<sub>x</sub> species: TPD and DRIFTS

#### 3.2.1. Pd/Al<sub>2</sub>O<sub>3</sub>

TPD profiles obtained from the Al<sub>2</sub>O<sub>3</sub> support and the Pd/Al<sub>2</sub>O<sub>3</sub> catalyst after exposure to an NO + O<sub>2</sub> feed (500 ppm NO + 5% O<sub>2</sub>) at 50 °C are shown in figure 2. The desorption spectrum obtained from the bare Al<sub>2</sub>O<sub>3</sub> support, figure 2(a), is dominated by three main features: an NO desorption peak centered at 150 °C, an NO<sub>2</sub> desorption peak centered at 175 °C and a high-temperature feature at ~460 °C which yields a mixture of NO, NO<sub>2</sub> and O<sub>2</sub>. A further small NO<sub>2</sub> desorption peak was also observed at 285 °C. Addition of Pd to this support did not introduce any additional features to the TPD profile, as shown in figure 2(b). The only difference observed was a downward shift, by about 70 °C, of those peaks associated with high-temperature desorption.

The corresponding DRIFTS spectra obtained after exposure of Pd/Al<sub>2</sub>O<sub>3</sub> to NO + O<sub>2</sub> at 50 °C are shown in figure 3. Control spectra obtained from the support alone showed similar absorption bands. In the initial spectrum obtained at 50 °C, bands are observed at 1464

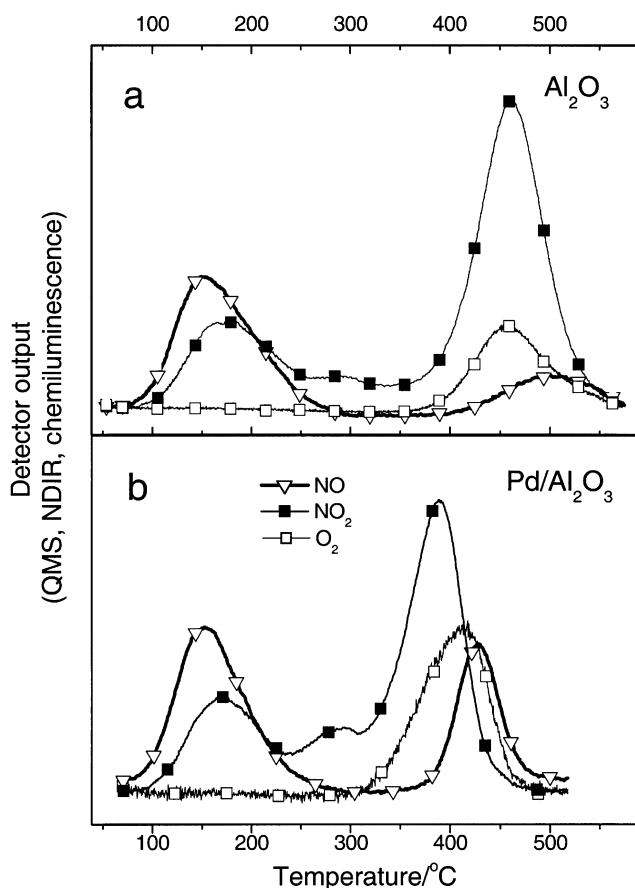


Figure 2. Temperature-programmed desorption spectra obtained from (a) Al<sub>2</sub>O<sub>3</sub> and (b) Pd/Al<sub>2</sub>O<sub>3</sub> following exposure to 500 ppm NO + 5% O<sub>2</sub> at 50 °C.

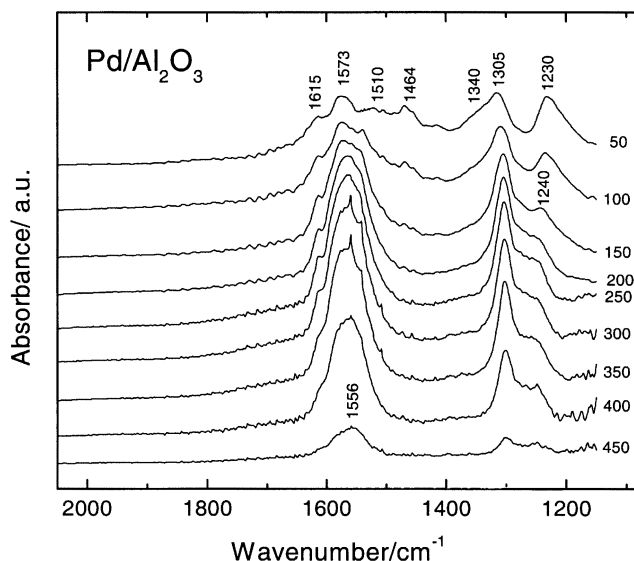


Figure 3. DRIFTS spectra obtained as a function of temperature following exposure of Pd/Al<sub>2</sub>O<sub>3</sub> to 500 ppm NO + 5% O<sub>2</sub> at 50 °C. Acquired in flowing helium with each temperature maintained for 20 min prior to recording spectra.

and 1230 cm<sup>-1</sup> that are assigned to linear and bridged nitrites, respectively [16], whilst the bands at 1510/1330 cm<sup>-1</sup> are assigned to a monodentate nitro (N-coordinated) species [16]. All these bands are extinguished between 100 and 150 °C and are therefore related to the low-temperature NO and NO<sub>2</sub> desorption peaks observed in TPD. The bands at 1615–1550 and 1305–1225 cm<sup>-1</sup> may be assigned with confidence to variously coordinated nitrates [16–18]. These species show high thermal stability, decomposing at temperatures above ~350 °C to yield the NO, NO<sub>2</sub> and O<sub>2</sub> observed in TPD. The downward shift in the temperature observed for nitrate decomposition in the presence of palladium, as shown in figure 2(b), perhaps indicates that at ~390 °C these nitrate species become relatively mobile on the Al<sub>2</sub>O<sub>3</sub> surface, migrating to Pd centers where their decomposition occurs.

It is important to note that no bands clearly attributable to NO<sub>x</sub> species adsorbed on palladium sites are observed in figure 3 [19,20]. This is in agreement with the TPD results which show that no additional features appear in the desorption profile when Pd is added to alumina, confirming that there is very little interaction between adsorbed NO<sub>x</sub> species and the palladium component of oxidized Pd/Al<sub>2</sub>O<sub>3</sub>.

#### 3.2.2. Pd/TiO<sub>2</sub>

TPD spectra obtained from TiO<sub>2</sub> and from the Pd/TiO<sub>2</sub> catalyst are shown in figures 4(a) and (b) respectively. The bare TiO<sub>2</sub> support gave two NO<sub>2</sub> desorption features, a small peak centered at 160 °C and a larger peak at 380 °C. The 380 °C feature is also associated with liberation of oxygen. In the presence of Pd, the high-temperature desorption feature is again shifted

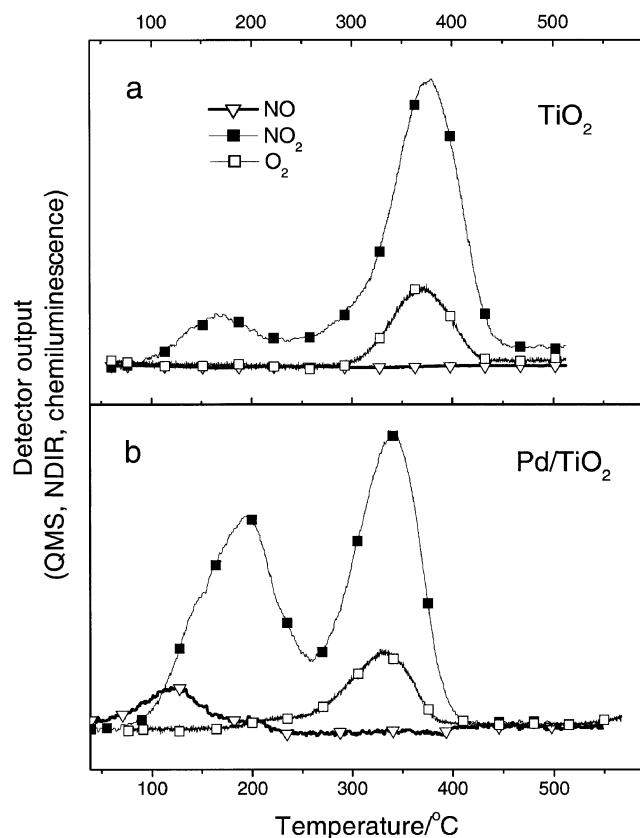


Figure 4. Temperature-programmed desorption spectra obtained from (a) TiO<sub>2</sub> and (b) Pd/TiO<sub>2</sub> following exposure to 500 ppm NO + 5% O<sub>2</sub> at 50 °C.

toward lower temperature, by approximately 50 °C in this case. More significantly, in marked contrast to the Al<sub>2</sub>O<sub>3</sub> system, addition of palladium to TiO<sub>2</sub> *does* result in the appearance of new features into the desorption profile observed following exposure to NO + O<sub>2</sub>. A new NO desorption feature is observed at 125 °C—note that this is completely absent from the bare TiO<sub>2</sub> data. An additional NO<sub>2</sub> desorption feature is also observed at 190 °C, with the 160 °C NO<sub>2</sub> desorption peak observed on TiO<sub>2</sub> now seen as a shoulder.

The corresponding DRIFTS spectra are shown in figures 5(a) and (b) respectively. The bands at 1614–1550 and 1250–1220 cm<sup>-1</sup> (not resolved) observed on TiO<sub>2</sub>, figure 5(a), are assigned to variously coordinated (bridging and bidentate) nitrates [21–24]. This assignment is again consistent with the high thermal stability of these species. The decomposition of these nitrates at temperatures above 250 °C results in the high-temperature NO and O<sub>2</sub> desorption observed in figure 4. The bands at 1500 and 1287 cm<sup>-1</sup> are assigned to a monodentate nitrate species [23] which desorbs at lower temperature and is responsible for the 150 °C NO<sub>2</sub> desorption feature observed in TPD (figure 4(a)).

In the presence of palladium, figure 5(b), new bands are observed at 1868 and 1819 cm<sup>-1</sup> which are assigned to Pd<sup>2+</sup>–NO species [25,26]. These species are responsible

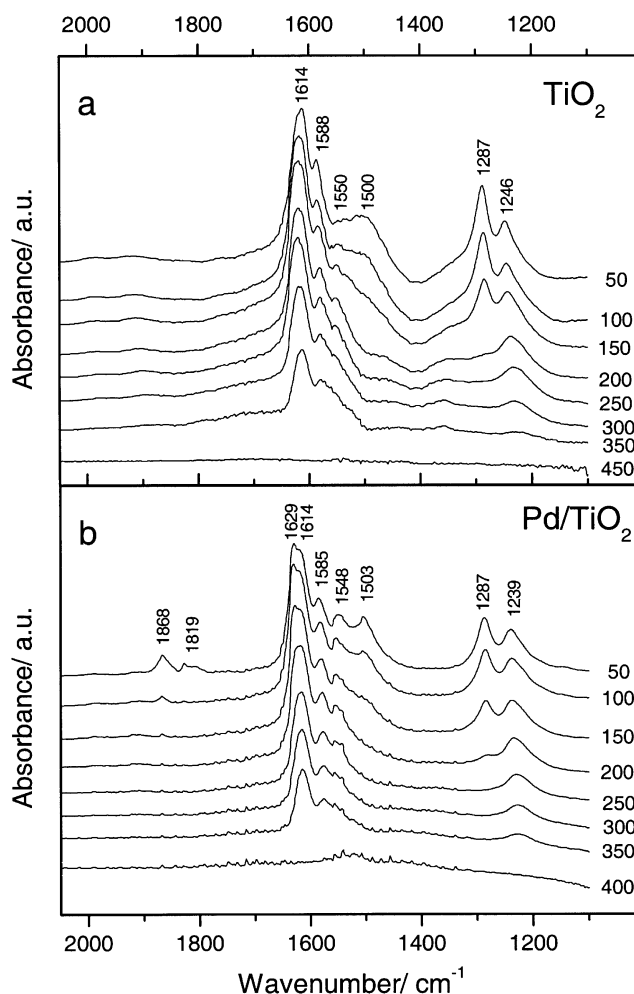


Figure 5. DRIFTS spectra obtained as a function of temperature following exposure of (a) TiO<sub>2</sub> and (b) Pd/TiO<sub>2</sub> to 500 ppm NO + 5% O<sub>2</sub> at 50 °C. Acquired in flowing helium with each temperature maintained for 20 min prior to recording spectra.

for the 125 °C NO desorption feature observed over Pd/TiO<sub>2</sub> (figure 4(b)). New features also appear at 1629, 1548 and 1503 cm<sup>-1</sup> and although their assignment is unclear, all are extinguished below 200 °C and are therefore likely to be associated with the 190 °C NO<sub>2</sub> desorption feature observed in TPD (figure 4(b)). These bands may be associated with nitrate species adsorbed at the metal/support interface, which would account for their lower thermal stability. Verykios *et al.* observed similar features in the Rh/TiO<sub>2</sub> system, which they tentatively assigned to various bridging nitrates coordinated to both Rh and Ti [24].

### 3.3. Adsorbed species present under reaction conditions: *in situ* DRIFTS

#### 3.3.1. Pd/Al<sub>2</sub>O<sub>3</sub>

The influence of hydrogen on the adsorbed species present on Pd/Al<sub>2</sub>O<sub>3</sub> is illustrated in figure 6. DRIFTS spectra obtained in flowing NO + O<sub>2</sub> (500 ppm

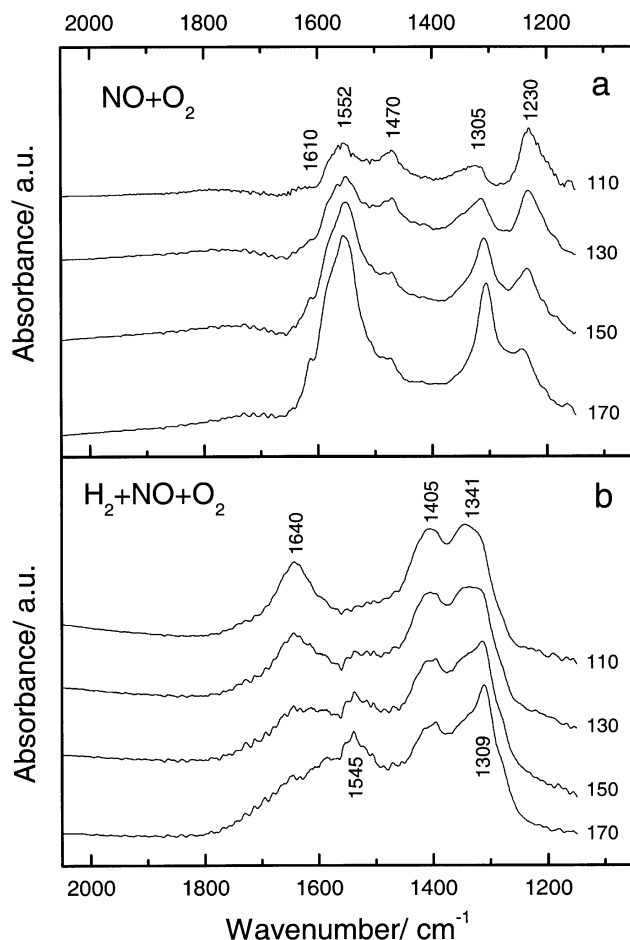


Figure 6. DRIFTS spectra obtained at various temperatures in a flow of (a) 500 ppm NO + 5% O<sub>2</sub> and (b) 4000 ppm H<sub>2</sub> + 500 ppm NO + 5% O<sub>2</sub> over Pd/Al<sub>2</sub>O<sub>3</sub>.

NO + 5% O<sub>2</sub>) over a range of temperatures are shown in figure 6(a), whilst the corresponding spectra taken in the presence of H<sub>2</sub> (4000 ppm H<sub>2</sub> + 500 ppm NO + 5% O<sub>2</sub>) are shown in figure 6(b). At 100 °C in flowing NO + O<sub>2</sub> bands due to variously coordinated nitrates (1552/1305 cm<sup>-1</sup>), linear nitrites (1470 cm<sup>-1</sup>) and bidentate nitrites (1230 cm<sup>-1</sup>) are observed as discussed previously. As the temperature is raised the nitrite species are removed whilst the intensity due to the nitrate species increased. When hydrogen was added to the gas mix new bands appeared at 1640, 1405 and 1341 cm<sup>-1</sup>. The band at 1640 cm<sup>-1</sup> is assigned to the deformation mode of adsorbed water [27] whilst those at 1405 and 1341 cm<sup>-1</sup> are assigned to water-solvated nitrate species. Identical bands were observed by Goodman *et al.* following exposure of HNO<sub>3</sub>-saturated Al<sub>2</sub>O<sub>3</sub> to water vapor [28]. Bands due to alumina-bound nitrites are not observed in the presence of H<sub>2</sub>. The bands due to coordinated nitrates (1545 and 1306 cm<sup>-1</sup>) are only apparent at higher temperatures (150 and 170 °C), where the concentration of adsorbed H<sub>2</sub>O is reduced.

With this support, no evidence was found for the presence of reduced palladium sites (Pd<sup>0</sup>) under reaction

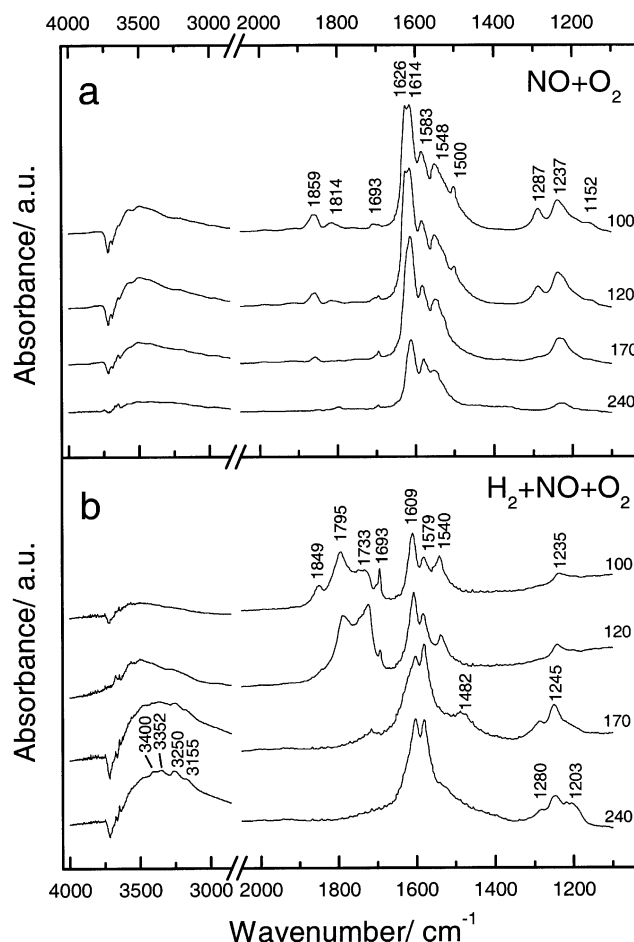


Figure 7. DRIFTS spectra obtained at various temperatures in a flow of (a) 500 ppm NO + 5% O<sub>2</sub> and (b) 4000 ppm H<sub>2</sub> + 500 ppm NO + 5% O<sub>2</sub> over Pd/TiO<sub>2</sub>.

conditions. This is in contrast to the results obtained with the corresponding Pd/TiO<sub>2</sub> catalyst as discussed below. Therefore the low activity of the Pd/Al<sub>2</sub>O<sub>3</sub> sample is indeed likely to be due to the fact that palladium remains predominantly in an oxidized state on this support. This may be due to stabilization of oxidized Pd species due to a strong interaction with Al<sub>2</sub>O<sub>3</sub>, possibly with formation of an aluminate phase [29].

### 3.3.2. Pd/TiO<sub>2</sub>

Spectra obtained from Pd/TiO<sub>2</sub> in the presence of flowing NO + O<sub>2</sub> (500 ppm NO + 5% O<sub>2</sub>) at various temperatures are shown in figure 7(a). As discussed above, bands due to variously coordinated bridging and bidentate nitrates (1626–1548 and 1220–1250 cm<sup>-1</sup>) and monodentate nitrate (1500/1287 cm<sup>-1</sup>) are observed in addition to the Pd<sup>2+</sup>–NO species (1859 and 1814 cm<sup>-1</sup>). In these experiments, where gaseous NO is present, an additional band is observed at 1693 cm<sup>-1</sup>, which may be assigned to the bent Pd–NO<sup>-</sup> species, while the weak band at 1152 cm<sup>-1</sup> is assigned to a NO<sup>-</sup> species [22]. The monodentate nitrate bands disappear

between 120 and 170 °C whilst the Pd<sup>2+</sup>–NO bands are not observed above 170 °C.

The influence of added H<sub>2</sub> (4000 ppm H<sub>2</sub> + 500 ppm NO + 5% O<sub>2</sub>) is illustrated in figure 7(b). No bands due to monodentate nitrate species are observed in the presence of H<sub>2</sub>, indicating that these species are relatively reactive and easily reduced by hydrogen. However, this is also observed on the bare TiO<sub>2</sub> support (data not shown), and as TiO<sub>2</sub> is a poor catalyst for the H<sub>2</sub>/NO/O<sub>2</sub> reaction, turnover of these nitrates cannot account for the observed high activity of Pd/TiO<sub>2</sub> (figure 1(a)).

At 100 °C, in addition to the Pd<sup>2+</sup>–NO band at 1849 cm<sup>-1</sup>, bands associated with linear Pd<sup>+</sup>–NO [30,31] and Pd<sup>0</sup>–NO [30–38] species are observed at 1795 and 1733 cm<sup>-1</sup> respectively. The band at 1693 cm<sup>-1</sup> is assigned to a bent Pd–NO<sup>-</sup> species [30–32,36,37]. The presence or absence of bridged NO on palladium (1570–1500 cm<sup>-1</sup> [19]) cannot be established due to interference from nitrate bands in this region. At 120 °C the band at 1849 cm<sup>-1</sup> is reduced in intensity whilst the linear Pd<sup>0</sup>–NO band at 1733 cm<sup>-1</sup> increases. These results clearly indicate reduction of palladium under reaction conditions. Therefore we may conclude that the high activity of Pd/TiO<sub>2</sub> in the temperature region where H<sub>2</sub> conversion approaches 100% (110 °C, figure 1(a)) is due to the adsorption of NO on reduced Pd sites. This process is followed by NO dissociation and subsequent recombination of two N<sub>(a)</sub> atoms to yield N<sub>2</sub> and/or reaction of N<sub>(a)</sub> with NO to produce N<sub>2</sub>O.

At 170/240 °C, the 1540 cm<sup>-1</sup> nitrate band is very much reduced in intensity in the presence of H<sub>2</sub>, indicating that this species (a bidentate nitrate) may also be relatively reactive. However, this behavior was also observed when flowing H<sub>2</sub> + NO + O<sub>2</sub> over bare TiO<sub>2</sub>, which we find to be relatively inactive for NO<sub>x</sub> reduction in this temperature range. Therefore this nitrate is not responsible for the second, high-temperature NO<sub>x</sub> reduction pathway observed on Pd/TiO<sub>2</sub> at ~240 °C (figure 1(a)).

Of more significance are new bands observed above 170 °C at ~1203/1280 cm<sup>-1</sup> and in the 3400–3100 cm<sup>-1</sup> region. These are assigned to symmetric deformation and NH stretching modes respectively of NH<sub>3</sub> species [21,39–41]. The splitting of these modes is assigned to NH<sub>3</sub> adsorbed on two types of Lewis acid sites [21,40]. The corresponding asymmetric deformation mode occurs at ~1600 cm<sup>-1</sup>, which is not clearly resolved due to overlap with strong nitrate bands in this region. The assignment of the 1482 cm<sup>-1</sup> band observed at 170 °C is unclear. A similar band observed by Ramis *et al.* following NO and NH<sub>3</sub> co-adsorption on V<sub>2</sub>O<sub>5</sub>–TiO<sub>2</sub> was tentatively assigned to a nitrosamide species (NH<sub>2</sub>NO) [42]. The broad shoulder extending down to 1400 cm<sup>-1</sup> in the spectrum obtained at 240 °C may indicate the presence of NH<sub>4</sub><sup>+</sup> species, as these are normally associated with a broad band centered at 1450 cm<sup>-1</sup>. In

light of the known high activity of NH<sub>3</sub> for NO<sub>x</sub> reduction under lean conditions, it is likely that it is the formation and subsequent conversion of these NH<sub>x</sub> species that is responsible for the high-temperature NO<sub>x</sub> conversion pathway observed on Pd/TiO<sub>2</sub> catalysts.

#### 4. Conclusions

1. The H<sub>2</sub>/NO/O<sub>2</sub> reaction under lean-burn conditions over a Pd/TiO<sub>2</sub> catalyst delivers very high NO<sub>x</sub> conversions (70–80%), comparable to the performance of platinum-based catalysts under these conditions [12]. In contrast, Pd/Al<sub>2</sub>O<sub>3</sub> was found to have very low activity for this reaction.
2. The Pd/TiO<sub>2</sub> catalyst displayed two separate NO<sub>x</sub> reduction pathways. These operate at different temperatures and therefore greatly extend the temperature range over which this catalyst is active for NO<sub>x</sub> reduction.
3. The low-temperature (~100 °C) NO reduction pathway observed over Pd/TiO<sub>2</sub> involves adsorption and subsequent dissociation of NO on reduced Pd sites. The low activity of Pd/Al<sub>2</sub>O<sub>3</sub> is a consequence of palladium remaining in an oxidized state under reaction conditions.
4. The high-temperature (~240 °C) NO reduction channel found with Pd/TiO<sub>2</sub> proceeds via NH<sub>x</sub> intermediates. The subsequent reaction of these with NO<sub>x</sub> species yields both N<sub>2</sub> and N<sub>2</sub>O.

#### Acknowledgments

R.C. acknowledges the award of a Cambridge University Oppenheimer Research Studentship. Additional support from Johnson Matthey plc is also acknowledged. We thank one of the reviewers for a valuable suggestion concerning the high-temperature channel.

#### References

- [1] V.I. Pârvulescu, P. Grange and B. Delmon, *Catal. Today* 46 (1998) 233.
- [2] A. Fritz and V. Pitchon, *Appl. Catal. B* 13 (1997) 1.
- [3] G.T. Went, L.J. Leu, R.R. Rosin and A.T. Bell, *J. Catal.* 134 (1992) 492.
- [4] G. Busca, L. Lietti, G. Ramis and F. Berti, *Appl. Catal. B* 18 (1998) 1.
- [5] A. Obuchi, A. Ohi, M. Nakamura, A. Ogata, K. Mizuno and H. Obuchi, *Appl. Catal. B* 2 (1993) 71.
- [6] R. Burch, P.J. Millington and A.P. Walker, *Appl. Catal. B* 4 (1994) 65.
- [7] K. Yokota, M. Fukui and T. Tanaka, *Appl. Surf. Sci.* 121/122 (1997) 273.
- [8] B. Frank, G. Emig and A. Renken, *Appl. Catal. B* 19 (1998) 45.
- [9] A. Ueda, N. Takayuki, A. Masashi and T. Kobayashi, *Catal. Today* 45 (1998) 135.
- [10] R. Burch and M.D. Coleman, *Appl. Catal. B* 23 (1999) 115.
- [11] C.N. Costa, V.N. Stathopoulos, V.C. Belessi and A.M. Efstathiou, *J. Catal.* 197 (2001) 350.

- [12] N. Macleod and R.M. Lambert, *Appl. Catal. B* 35 (2002) 269.
- [13] A. Ueda, T. Nakao, M. Azuma and T. Kobayashi, *Chem. Lett.* (1998) 595.
- [14] S. Komai, T. Hattori and Y. Murakami, *J. Catal.* 120 (1989) 370.
- [15] N. Macleod, J. Isaac and R.M. Lambert, *J. Catal.* 193 (2000) 115.
- [16] W.S. Kijlstra, D.S. Brand, E.K. Poels and A. Blik, *J. Catal.* 171 (1997) 208.
- [17] F.C. Meunier, J.P. Breen, V. Zuzaniuk, M. Olsson and J.R.H. Ross, *J. Catal.* 187 (1999) 493.
- [18] S. Kameoka, Y. Ukisu and T. Miyadera, *Phys. Chem. Chem. Phys.* 2 (2000) 367.
- [19] N. Sheppard and C. De La Cruz, *Catal. Today* 70 (2001) 3.
- [20] T.E. Hoost, K. Otto and K.A. Laframboise, *J. Catal.* 155 (1995) 303.
- [21] T.J. Dines, C.H. Rochester and A.M. Ward, *J. Chem. Soc. Faraday Trans.* 87 (1991) 643.
- [22] K. Hadjiivanov and H. Knözinger, *Phys. Chem. Chem. Phys.* 2 (2000) 2803.
- [23] M.M. Kantcheva, V.Ph. Bushev and K.I. Hadjiivanov, *J. Chem. Soc. Faraday Trans.* 88 (1992) 3087.
- [24] T. Chafik, A.M. Efstathiou and X.E. Verykios, *J. Phys. Chem. B* 101 (1997) 7968.
- [25] C. Descorme, P. Gelin, C. Lecuyer and M. Primet, *J. Catal.* 177 (1998) 352.
- [26] M. Valden, R.L. Keiski, N. Xiang, J. Pere, J. Aaltonen, M. Pessa, T. Maunula, A. Savimaki, A. Lahti and M. Harkonen, *J. Catal.* 161 (1996) 614.
- [27] F. Radtke, R.A. Koeppel, E.G. Minardi and A. Baiker, *J. Catal.* 167 (1997) 127.
- [28] A.L. Goodman, E.T. Bernard and V.H. Grassian, *J. Phys. Chem. A* 105 (2001) 6443.
- [29] T.E. Hoost and K. Otto, *Appl. Catal. A* 92 (1992) 39.
- [30] T. Maillet, J. Barbier, P. Gelin, H. Praliaud and D. Duprez, *J. Catal.* 202 (2001) 367.
- [31] K. Almusaiter and S.S.C. Chuang, *J. Catal.* 184 (1999) 189.
- [32] N. Sheppard and C. De La Cruz, *Catal. Today* 70 (2001) 3.
- [33] A.J. Renouprez, J.F. Trillat, G. Bergeret, P. Delichere, J.L. Rousset, J. Massardier, D. Loffreda, D. Simon, F. Delbecq and P. Sautet, *J. Catal.* 198 (2001) 243.
- [34] A. El Hamdaoui, G. Bergeret, J. Massardier, M. Primet and A. Renouprez, *J. Catal.* 148 (1994) 47.
- [35] F.B. Noronha, M.A.S. Baldanza and M. Schmal, *J. Catal.* 188 (1999) 270.
- [36] A.M. Venezia, L.F. Liotta, G. Deganello, P. Terreros, M.A. Pena and J.L.G. Fierro, *Langmuir* 15 (1999) 1176.
- [37] K. Almusaiter and S.S.C. Chuang, *J. Catal.* 180 (1998) 161.
- [38] T.E. Hoost, K. Otto and K.A. Laframboise, *J. Catal.* 155 (1995) 303.
- [39] G. Ramis, G. Busca, V. Lorenzelli and P. Forzatti, *Appl. Catal.* 64 (1990) 243.
- [40] G. Ramis, L. Yi, G. Busca, M. Turco, E. Kotur and R.J. Willey, *J. Catal.* 157 (1995) 523.
- [41] N.Y. Topsøe, H. Topsøe and J.A. Dumesic, *J. Catal.* 151 (1995) 226.
- [42] G. Ramis, G. Busca, F. Bregani and P. Forzatti, *Appl. Catal.* 64 (1990) 259.